Lab on a Chip

View Online / Journal Homepage
Dynamic Article Links

Cite this: DOI: 10.1039/c2lc40074j

www.rsc.org/loc

PAPER

Human gut-on-a-chip inhabited by microbial flora that experiences intestinal peristalsis-like motions and flow†‡

Hyun Jung Kim,[a] Dongeun Huh,[a] Geraldine Hamilton[a] and Donald E. Ingber*[abc]

Received 18th January 2012, Accepted 5th March 2012
DOI: 10.1039/c2lc40074j

Published on 08 March 2012 on http://pubs.rsc.org | doi:10.1039/C2LC40074J
Downloaded by UNIVERSITY OF SOUTH AUSTRALIA on 08 May 2012

Development of an *in vitro* living cell-based model of the intestine that mimics the mechanical, structural, absorptive, transport and pathophysiological properties of the human gut along with its crucial microbial symbionts could accelerate pharmaceutical development, and potentially replace animal testing. Here, we describe a biomimetic 'human gut-on-a-chip' microdevice composed of two microfluidic channels separated by a porous flexible membrane coated with extracellular matrix (ECM) and lined by human intestinal epithelial (Caco-2) cells that mimics the complex structure and physiology of living intestine. The gut microenvironment is recreated by flowing fluid at a low rate (30 μL h^{-1}) producing low shear stress (0.02 dyne cm^{-2}) over the microchannels, and by exerting cyclic strain (10%; 0.15 Hz) that mimics physiological peristaltic motions. Under these conditions, a columnar epithelium develops that polarizes rapidly, spontaneously grows into folds that recapitulate the structure of intestinal villi, and forms a high integrity barrier to small molecules that better mimics whole intestine than cells in cultured in static Transwell models. In addition, a normal intestinal microbe (*Lactobacillus rhamnosus* GG) can be successfully co-cultured for extended periods (>1 week) on the luminal surface of the cultured epithelium without compromising epithelial cell viability, and this actually improves barrier function as previously observed in humans. Thus, this gut-on-a-chip recapitulates multiple dynamic physical and functional features of human intestine that are critical for its function within a controlled microfluidic environment that is amenable for transport, absorption, and toxicity studies, and hence it should have great value for drug testing as well as development of novel intestinal disease models.

Introduction

The drug development process has been severely hampered by the need for animal models that are costly, labor-intensive, time-consuming and questionable ethically.[1] Of even greater concern is that animal models often do not predict results obtained in humans,[2,3] and this is a particular problem when addressing challenges relating to metabolism, transport, and oral absorption of drugs and nutrients.[4,5] For these reasons, there has been increasing interest in development of *in vitro* models of human intestinal function, including cell culture systems that utilize Transwell filter inserts[6,7] which enable transepithelial barrier and transport studies,[8,9] and miniaturized microfluidic models that also support long-term culture.[10–14] Others have attempted to recreate the normal three-dimensional (3D) architecture of the intestinal lining *in vitro* by culturing human intestinal epithelial (*e.g.* Caco-2) cells on hydrogel substrates that were micro-engineered to mimic the shape, size and density of human intestinal villi.[11] However, none of the existing *in vitro* intestinal models recapitulate the mechanically active microenvironment of living intestine (peristaltic motions and intralumenal fluid flow) that is critical for normal organ physiology,[15] as well as for development of Crohn's disease and other intestinal disorders.[16–19] Another limitation of existing *in vitro* gut models is that it has not been possible to grow living microbes on the luminal surface of cultured intestinal epithelium for extended periods as normally occurs in living intestine. This is a key problem because microbial symbionts normally contribute significantly to intestinal barrier function, metabolism and absorption of drugs and chemicals, and many diseases.[20–24] Thus, in the present study, we explored whether we could leverage advances in microfluidic systems engineering recently used to develop a mechanically active 'human lung-on-a-chip' model that exhibits cyclic

[a]*Wyss Institute for Biologically Inspired Engineering at Harvard University, CLSB Bldg. 5th floor, 3 Blackfan Circle, Boston, MA 02115, USA. E-mail: don.ingber@wyss.harvard.edu; Fax: +617-432-7048; Tel: +617-432-7044*
[b]*Vascular Biology Program, Departments of Pathology and Surgery, Children's Hospital Boston and Harvard Medical School, Boston, MA 02115, USA*
[c]*School of Engineering and Applied Sciences, Harvard University, Cambridge, MA 02138, USA*

† Published as part of a LOC themed issue dedicated to research from the USA: Guest Editors Don Ingber and George Whitesides

‡ Electronic supplementary information (ESI) available. See DOI: 10.1039/c2lc40074j

breathing motions[25] to build a more physiologically relevant *in vitro* model of the human intestine in the form of a human 'gut-on-a-chip' that undergoes peristalsis, experiences fluid flow, and supports growth of microbial flora without compromising human cell viability.

Experimental

Microdevice design and fabrication

The gut-on-a-Chip device was fabricated from a flexible clear polydimethylsiloxane (PDMS; Sylgard, Dow Corning) polymer by adapting a soft lithography technique that was previously used to create a breathing lung-on-a-chip device with a similar architecture.[25] The aligned upper and lower microchannels were of same size (150 μm high × 1000 μm wide) and separated by a 30 μm thick PDMS membrane containing 10 μm diameter circular pores with a 25 μm spacing (center to center) (Fig. 1a–c). As shown in Fig. 2, the upper and lower microchannel layers were individually prepared by casting PDMS prepolymer (15 : 1 w/w ratio of PDMS to curing agent) on a microfabricated mold of the inverse channel design made of photoresist (SU-8 100, Microchem, Newton, MA).[26,27] The porous membrane (Fig. 1c, right inset) was prepared by casting PDMS prepolymer on a microfabricated silicon wafer containing post arrays with circular pillars (10 μm diameter × 30 μm high with 25 μm spacing; MEMS and Nanotechnology Exchange, Reson, VA), overlaying the prepolymer with a cured, flat, silanized PDMS support layer, placing a 3 kg weight on the setup, and curing the polymer at 60 °C for 12 h. After peeling the porous PDMS membrane and support layer from the wafer, the surface of the porous membrane was exposed to plasma generated by a laboratory corona treater (BD-20AC, Electro-Technic Products, Inc., Chicago, IL), as was the upper microchannel layer. The plasma-treated surfaces of the porous PDMS membrane and upper microchannel layer were then immediately placed in conformal contact. Incubation of the whole setup at 80 °C overnight resulted in irreversible bonding of the two PDMS layers. The PDMS support layer was then peeled off the bottom of the PDMS porous membrane and portions of this membrane located over the lateral vacuum chambers were torn off using forceps to make full-height hollow vacuum chambers. The exposed surface of the torn PDMS membrane and top surface of a lower PDMS microchannel layer with same shape to the upper layer were then exposed to plasma, aligned, pressed together under a stereoscope (Zeiss Discovery V20 Stereo Microscope, Carl Zeiss MicroImaging Gmb, Germany), and cured at 80 °C overnight to produce the entire bonded device containing hollow vacuum chambers on either side of the main microchannel (Fig. 1a & 2). Tubing (Tygon 3350 silicone tubing, ID 1/32″, OD 3/32″, Beaverton, MI) was connected from fluid medium and vacuum sources to the upper and lower microfluidic channels, respectively, using hub-free stainless steel blunt needles (18G; Kimble Chase, Vineland, NJ). This allowed us to control flow of culture medium within the central microchannel, and to regulate application of vacuum to the side chambers under computer control to exert cyclic mechanical strain to mimic peristaltic motions (Fig. 1d).

Cell culture

Human Caco-2 intestinal epithelial cells (Caco-2BBE human colorectal carcinoma line[28]) were obtained from the Harvard Digestive Disease Center and grown in Dulbecco's Modified Eagle Medium containing 4.5 g L^{-1} glucose (DMEM; Gibco, Grand Island, NY) supplemented with 20% fetal bovine serum (FBS; Gibco), 100 units mL^{-1} penicillin, 100 μg mL^{-1} streptomycin (Gibco), 100 μg mL^{-1} Normocin (Invivogen, San Diego, CA), and 25 mM HEPES. Antibiotics were removed from the culture medium for co-culture of Caco-2 cells with living intestinal microbes.

After microdevice fabrication and assembly, the tubing and microfluidic channels were sterilized by flowing 70% (v/v) ethanol through the device and drying the entire system in a 60 °C oven. The dried devices were then exposed to ultraviolet light and ozone (UVO Cleaner 342, Jelight Company Inc., Irvine, CA) simultaneously for 30 min. An ECM solution[29–31] containing rat type I collagen (50 μg mL^{-1}; Gibco) and Matrigel (300 μg mL^{-1}; BD Biosciences, Bedford, MA) in serum-free DMEM was injected into the microchannels and incubated at 37 °C for 2 h, after which the microchannels were perfused with culture medium. Caco-2 cells harvested with trypsin/EDTA solution (0.05%; Gibco) were plated on the top surface of the ECM-coated porous membrane (1.5×10^5 cells cm^{-2}) by gently pulling the cell solution into the upper microchannel using a sterile syringe (1 mL Tuberculin slip tip; BD, Franklin Lakes, NJ) and needle (25G 5/8; BD). At this cell density, neither aggregation nor superposition of cells was observed in the microchannel after seeding into the gut-on-a-chip device. Caco-2 cells attached to the ECM-coated PDMS surface within 30 min and generated cell-cell adhesions within 1 h (not shown). After 1 h, a syringe pump (BS-8000; Braintree Scientific Inc., Braintree, MA) was used to perfuse culture medium continuously through the upper microchannel at a constant flow rate (30 μL h^{-1}, which produces 0.02 dyne cm^{-2} shear stress) for the first day of culture to make sure that the Caco-2 cells established an intact monolayer, and then medium was flowed at a same rate through both the upper and lower channels thereafter.

To mechanically deform the Caco-2 monolayer in a cyclic manner that mimics peristaltic motions of the intestine, cyclic suction was applied to tubing connected to the vacuum chambers (Fig. 1a,b) using a computer-controlled FX5K Tension instrument (Flexcell International Corporation, Hillsborough, NC). This device is capable of unidirectional elongation of the porous membrane in gut-on-a-chip by up to ~50%; however, we applied a cyclic stretching regimen (10% mean cell strain, 0.15 Hz frequency) that more closely mimics the mechanical microenvironment that epithelial cells experience in the living human intestine *in vivo*[16,32] in these studies. The relation between applied pressure, distortion of the porous membrane substrate and cell deformation was first quantified over a broad range (0 to ~30% strain) to characterize the control parameters of the device (Fig. 1e).

We also carried out control studies using static cultures of Caco-2 cells in Transwell plates (Corning Inc., Lowell, MA) containing porous polyester membrane inserts (0.33 cm^2, 0.4 μm pores) that were pre-coated with the same ECM mixture of type I collagen and Matrigel used in the gut-on-a-chip device. Caco-2

Published on 08 March 2012 on http://pubs.rsc.org | doi:10.1039/C2LC40074J
Downloaded by UNIVERSITY OF SOUTH AUSTRALIA on 08 May 2012

This journal is © The Royal Society of Chemistry 2012

Published on 08 March 2012 on http://pubs.rsc.org | doi:10.1039/C2LC40074J
Downloaded by UNIVERSITY OF SOUTH AUSTRALIA on 08 May 2012

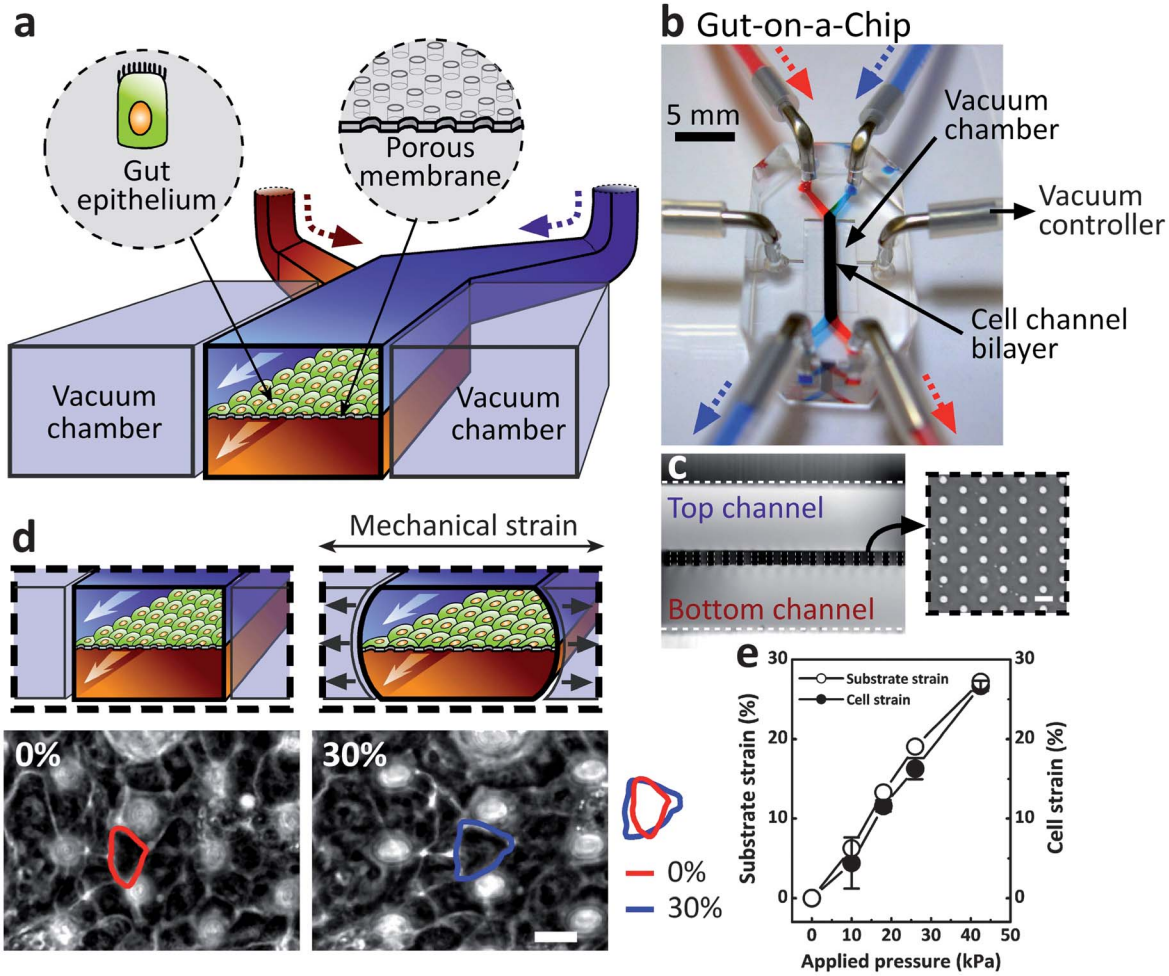


Fig. 1 The human gut-on-a-chip. (**a**) A schematic of the gut-on-a-chip device showing the flexible porous ECM-coated membrane lined by gut epithelial cells cross horizontally through the middle of the central microchannel, and full height vacuum chambers on both sides. (**b**) A photographic image of the gut-on-a-chip device composed of clear PDMS elastomer. A syringe pump was used to perfuse (direction indicated by arrows) blue and red dyes through tubing to the upper and lower microchannels, respectively, to visualize these channels. (**c**) A cross-sectional view of the top and bottom channels (both 150 μm high) of the gut-on-a-chip; square inset shows a top view of a portion of the porous membrane (10 μm pores; bar, 20 μm). (**d**) Schematics (top) and phase contrast images (bottom) of intestinal monolayers cultured within the gut-on-a-chip in the absence (left) or presence (right) of mechanical strain (30%; arrow indicated direction) exerted by applying suction to the vacuum chambers. Red and blue outlines indicate the shape of a single Caco-2 cell before (red) and after (blue) mechanical strain application (bar, 20 μm). Note that the cell distorts in the direction of the applied tension. The regular array of small white circles are pores visible beneath the epithelial monolayer. (**e**) Quantitation of the mechanical strain produced in the ECM-coated, flexible, porous PDMS membrane (open circles) and in the adherent gut epithelial cells (closed circles) as a function of pressure applied by the vacuum controller.

cells also were plated at the same density (1.5×10^5 cells cm^{-2}) with medium being refreshed every other day to both the apical and basolateral side of the Transwell chamber.

Epithelial barrier measurements

The integrity of the human intestinal epithelial cell monolayer resulting from establishment of apical tight junctions was evaluated by staining for the tight junction protein, occludin,[33] using confocal immunofluorescence microscopy and by measuring transepithelial electrical resistance (TEER). In Transwell cultures, TEER was measured using a Millicell ERS meter (Millipore, Bedford, MA) coupled to a chopstick-like electrode, and TEER values (Ω cm^2) were determined by subtracting the baseline resistance value measured in the absence of cells and then multiplying the remaining 'specific' resistance value (Ω) times the cell culture surface area (cm^2). The TEER of the Caco-2 monolayer cultured in the gut-on-a-chip was measured using a voltage-ohm meter (87V Industrial Multimeter, Fluke Corporation, Everett, WA) coupled to Ag/AgCl electrode wires (0.008″ in diameter; A-M Systems, Inc., Sequim, WA); control studies confirmed that similar TEER results were obtained with both methods. Again, the baseline resistance value measured in the absence of cells was subtracted from results obtained with the Caco-2 monolayer, and specific TEER values were determined by multiplying the specific resistance times the total cell culture surface area on the PDMS membrane (Table S1).

Published on 08 March 2012 on http://pubs.rsc.org | doi:10.1039/C2LC40074J
Downloaded by UNIVERSITY OF SOUTH AUSTRALIA on 08 May 2012

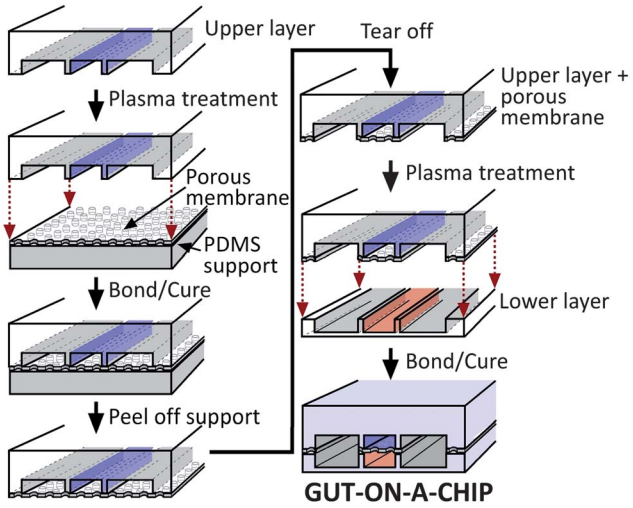


Fig. 2 Microfabrication process. The gut-on-a-chip microdevice fabricated from three PDMS layers (an upper layer, a porous membrane, and a lower layer), which were sequentially bonded and modified to create the central cell culture channel with upper (blue) and lower (orange) channels, and two lateral vacuum chambers. The regions of the porous PDMS membrane that spanned the vacuum chambers (grey) were physically torn off during the process to create full height chambers. See text for a detailed step-by-step description of methods.

Measurement of aminopeptidase activity

Human intestinal epithelial cell functionality was measured by quantitating the specific activity of an apical brush border aminopeptidase enzyme that is expressed by differentiated human intestinal Caco-2 cell monolayers[34] using L-alanine-4-nitroanilide hydrochloride (A4N; Sigma, St. Louis, MO) as a substrate. In Transwell studies, A4N substrate solution (1.5 mM in medium) was applied to the top chamber of cells cultured for 5 or 21 days and after incubation at 37 °C for 2 h, the solution (70 μL) in the top chamber was transferred to a 96 well plate (Black/clear flat bottom, BD Falcon, Franklin Lakes, NJ) where the cleavage product (*i.e.* 4-nitroaniline) was quantified in a microplate reader (SpectraMax M5, Molecular Devices, Sunnyvale, CA) at 405 nm using culture medium as a reference. The specific activity of aminopeptidase was obtained by dividing the total activity by the total cell number. The actual amount of cleaved product was estimated based on the calibration curve of 4-nitroaniline.

To measure the specific activity of aminopeptidases in the gut-on-a-chip, the A4N solution was flowed at 30 μL h^{-1} through the upper microchannel of the device containing a Caco-2 monolayer cultured in the presence or absence of cyclic mechanical strain (10% strain, 0.15 Hz in frequency) for 5 days. Samples (30 μL) collected every hour from the outlet of the upper microchannel were diluted to the same volume (70 μL) that was used to analyze the Transwell samples and transferred to a 96 well plate (Black/clear flat bottom, BD Falcon) where optical densities were measured as described above.

Paracellular permeability measurements

The apparent permeability coefficient (P_{app}, cm s^{-1}) of the intestinal cell monolayer was determined after tight junctional integrity was established (TEER ≥ 600 Ω cm^2) by measuring the transport of fluorescein isothiocyanate (FITC)-labeled dextran (FD20; 20 kDa; Sigma, St. Louis, MO) over time. In Transwell studies, the FD20 was applied (200 μL; 1 mg mL^{-1}) to the apical surface of the epithelium in the top chamber, and aliquots (70 μL) were removed from the lower chamber every 15 min (700 μL total volume) while simultaneously replenishing with the same volume of fresh culture medium. Fluorescence intensity (490 nm excitation/520 nm emission) of the samples collected from the lower chamber were measured immediately to quantify the amount of FD20 transported from the apex to the basolateral surface of the cell. After subtracting the baseline fluorescence value measured in culture medium alone, the apparent permeability coefficient (P_{app}) was calculated according to P_{app} (cm s^{-1}) = $(dQ/dt)(1/AC_o)$ where dQ/dt is the steady-state flux (g s^{-1}), A is the culture surface area (cm^2) and C_o is the initial concentration (mg mL^{-1}) of the FD20 solution applied to the apical cell surface.[35]

In studies carried out using the gut-on-a-chip, the FD20 solution was perfused through the upper channel, and sample aliquots (30 μL) collected every hour from the outlet of a lower channel were analyzed to quantitate the amount of FD20 that was transported across the Caco-2 paracellular barrier. The Caco-2 monolayer in the microchannel was cultured in the presence of medium flow (30 μL h^{-1}), with or without exposure to cyclic mechanical strain (10% strain, 0.15 Hz in frequency) for 5 days.

Microbial studies

To study physiologically relevant human intestinal epithelial cell-microbe interactions, we used a strain of *Lactobacillus rhamnosus* GG (LGG) obtained from American Type Culture Collection (ATCC 53103; Manassas, VA) that was originally isolated from human gut.[36] LGG cells were grown in autoclaved Lactobacilli MRS broth (BD Diagnostic, Sparks, MD) in a humidified incubator (37 °C, 5% CO_2) without shaking overnight prior to transfer to the apical surface of Caco-2 cell monolayers that were pre-cultured for ~4–5 days to developed relevant intestinal barrier integrity (TEER ≥ 600 Ω cm^2). The cell culture medium was switched to antibiotic-free medium for 12 h prior to seeding of the LGG cells (~1.0×10^7 CFU mL^{-1}, final cell density). LGG cells placed on the apical surface of Caco-2 cells in Transwell cultures were incubated for 1.5 h, carefully washed free of non-adherent LGG cells with antibiotic-free culture medium, and incubated in the same medium for extended culture as indicated. The same method was used for studies in the gut-on-a-chip, except that after the attachment period, antibiotic-free medium was perfused through both upper and lower microchannels at 40 μL h^{-1} with the cyclic stretching (10% strain, 0.15 Hz in frequency).

Microbial β-galactosidase activity measurements

To analyze the viability and function of LGG cells in co-culture studies, the catalytic activity of LGG β-galactosidases was determined by measuring the ability of the cultured microbes to cleave the enzyme substrate, *O*-nitrophenyl β-D-galactopyranoside (ONPG; Sigma, St. Louis, MO). For these studies, LGG and

 This journal is © The Royal Society of Chemistry 2012

Published on 08 March 2012 on http://pubs.rsc.org | doi:10.1039/C2LC40074J
Downloaded by UNIVERSITY OF SOUTH AUSTRALIA on 08 May 2012

Caco-2 cells were co-cultured in the gut-on-chip and perfused (40 μL h^{-1}) with antibiotic-free medium for 48 h before 30 μg mL^{-1} ONPG was added to the medium. Samples (30 μL) collected every hour from the outlet of the upper microchannel were analyzed by measuring optical density (420 nm) using a SpectraMax M5 instrument (Molecular Devices, Sunnyvale, CA) to quantify the amount of product (*i.e. O*-nitrophenol) released by β-galactosidases in the LGG cells. The amount of cleaved product was estimated based on the calibration curve of *O*-nitrophenol.

Morphological studies

Cell images were recorded during culture using a Moticam 2500 camera (Motic China Group Co., Ltd.) with imaging software (Motic images plus 2.0; Motic China Group Co., Ltd.) on a Zeiss Axiovert 40CFL phase contrast microscope. To visualize cell shape and polarity, F-actin, nuclei, and mucin were stained in Caco-2 cell monolayers that were fixed in 4% (v/v) paraformaldehyde and permeabilized in 0.3% (v/v) Triton-X-100 (Sigma, St. Louis, MO) using FITC-phalloidin (Sigma, St. Louis, MO), 4′,6-diamidino-2-phenylindole, dihydrochloride (DAPI; Molecular Probe, Eugene, OR), and anti-mucin 2 antibodies[37] (mouse monoclonal antibody; abcam, Cambridge, MA), respectively. Following fluorescence staining, the cells were scanned using an inverted laser scanning confocal microscope (Leica SP5 X MP, Germany) equipped with a photomultiplier tube and coupled to a 405 nm laser and a white light laser (489–670 nm). To visualize epithelial tight junctions, immunofluorescence staining was performed using anti-occludin antibodies (mouse monoclonal antibody-Alexa Fluor 594; Molecular Probe, Eugene, OR), and samples were visualized on a Zeiss Axio Observer Z1 *epi*-fluorescence microscope coupled to a CCD camera (CoolSNAP HQ^2, 1392 × 1040 resolution; Photometrics, Tucson, AZ); computerized image analysis of recorded images was carried out using MetaMorph image software (Molecular Devices).

Statistical analysis

All results are expressed as mean ± standard error (SEM). For the statistical evaluation of quantified data, a one-way analysis of variance (ANOVA) with Tukey-Kramer multiple comparisons test was performed using GraphPad InStat version 3.10 (GraphPad Software Inc., San Diego CA). Differences were considered statistically significant when $p < 0.05$.

Results and discussion

Gut-on-a-chip microsystem design

The gut-on-a-chip microdevice was designed to mimic the dynamic mechanical microenvironment of the gut, support perfusion-based long-term cell culture with microbial symbionts, and enable analysis of intestinal epithelial barrier functions *in vitro*. To accomplish these goals, the microsystem design incorporated two layers of closely apposed microfluidic channels separated by a thin porous membrane coated with ECM and lined by human Caco-2 intestinal epithelial cells (Fig. 1a). Culture medium was perfused through both microchannels at 10–100 μL h^{-1} (0.006–0.06 dyne cm^{-2}) to mimic fluid flow and shear stresses of the human intestine, which have previously been shown to be ~0.002–0.08 dyne cm^{-2}.[38–40] To create rhythmic mechanical deformations of the epithelial cell monolayer similar to those caused by peristaltic motions of the human intestine, cyclic suction regulated by a computer-controlled vacuum manifold was applied to the full-height, hollow, vacuum chambers positioned on either side of the microchannels to repeatedly stretch and relax the elastic, ECM-coated porous membrane (Fig. 1d). Phase contrast microscopic analysis of cell shape in human intestinal epithelial monolayers grown under these conditions confirmed that both substrate distortion and cell deformation increased linearly from 0 to 30% as the level of suction pressure was raised from 0 to 45 kPa (Fig. 1d,e).

Impact of mimicking the gut microenvironment on epithelial organization

To explore the physiological relevance of mimicking the physical microenvironment of the intestine, Caco-2 cells were grown either in a static Transwell chamber without fluid flow and mechanical strain (Fig. 3a) or in the gut-on-a-chip microfluidic device with either flow alone (Fig. 3b) or flow plus cyclic mechanical strain (Fig. 3c). Caco-2 cells commonly must be grown in the Transwell system for at least 3 weeks to exhibit differentiated intestinal barrier functions, and thus we analyzed cells at 21 days in these static cultures. In preliminary studies, we noticed that well-defined epithelial monolayers formed much more quickly in the microfluidic device, and hence, we were able to carry out studies comparing epithelial monolayer functions with the Transwell cultures after only 3 days of culture in the microfluidic system.

Phase contrast and immunofluorescence microscopic studies using antibodies directed against the tight junction protein, occludin, confirmed that Caco-2 cells formed confluent polygonal epithelial monolayers with well developed tight junctions under all three culture conditions, even though cells in the microdevice were cultured for a much shorter time (Fig. 3a–c). However, confocal fluorescence microscopic analysis of F-actin distribution and nuclear position revealed that epithelial cells grown under static conditions in the Transwell were highly flattened and almost squamous in form (Fig. 3a). In contrast, cells grown in the presence of fluid flow at a rate (30 μL h^{-1}; 0.02 dyne cm^{-2} shear stress) with or without concomitant cyclic strain were almost 6-fold taller in size (Fig. 3d) and hence, exhibited polarized epithelial cell forms with basal nuclei (Fig. 3b,c). In fact, cells under fluid flow were about the same columnar shape and size (30–40 μm high) that has been reported for cells within healthy intact human intestinal epithelium *in vivo*.[41]

One possibility is that this effect on cell morphology could be an artifact of placement within a microchannel device compared with a Transwell chamber. However, when we lowered the fluid flow rate in the microfluidic channel to a minimal level (10 μL h^{-1}), the cells failed to increase in height and looked much like they did in the static Transwell system[42] (Fig. 3a), whereas increasing the rate to 100 μL h^{-1} had no additive effect beyond what we observed at 30 μL h^{-1} (Fig. S1). Thus, application of physiological fluid flow and shear stress across the apical surface of the intestinal epithelium accelerates cell differentiation as

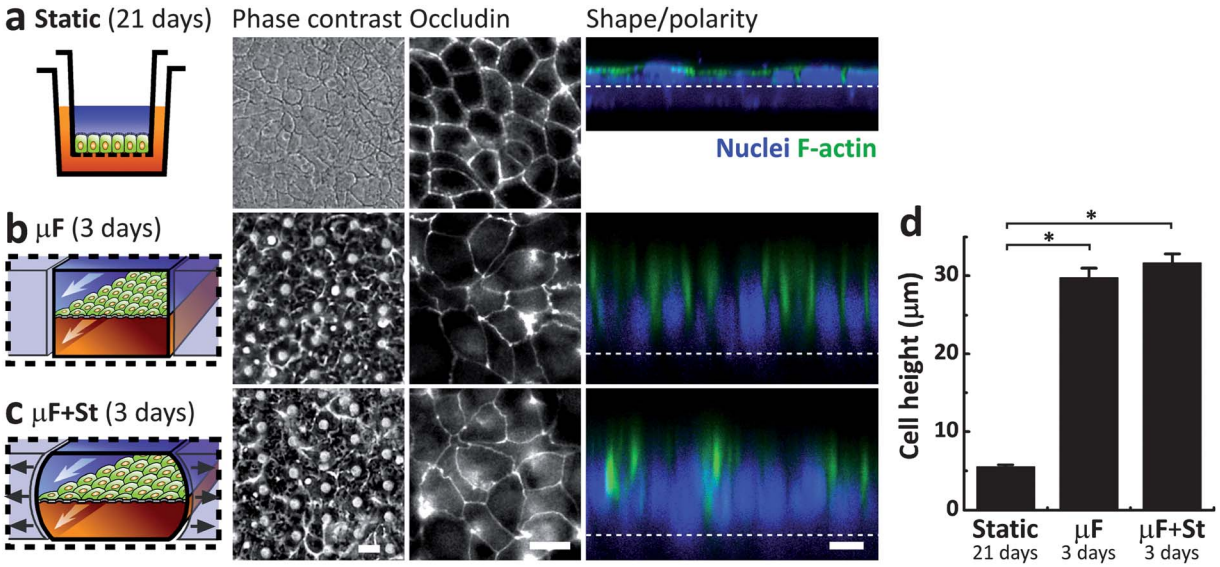


Fig. 3 Morphology of the Caco-2 epithelial cells cultured in the static Transwell system for 21 days (**a**) *versus* in the gut-on-a-chip with microfluidic flow (30 μL h^{-1}; μF) without (**b**) or with (**c**) application of cyclic mechanical strain (10%; 0.15Hz; μF + St) for 3 days. Schematics (left) show the system layout; fluorescence views (center) show the distribution of the tight junction protein, occludin, in the epithelial monolayers; and the confocal fluorescence views (right) show of a vertical cross section of the epithelium highlighting cell shape and polarity (nuclei in blue and F-actin in green). The regular array of small white circles in (b) and (c) are pores visible beneath the epithelial monolayer; the dashed white line indicates top of anchoring substrate (bar, 20 μm). (**d**) The average height of Caco-2 cells grown in static Transwell cultures or the microfluidic gut-on-a-chip without (μF) or with (μF + St) mechanical strain (* $p < 0.001$).

measured by an increase in height and polarization of these cells within 3 days of culture under conditions where cells in the Transwell systems remained flat even after 3 weeks. Moreover, flow or shear stress was the critical determinant of this response as cyclic strain did not produce any significant additive effect (Fig. 3d).

Interestingly, when Caco-2 cells were cultured in the gut-on-a-chip microdevice with flow and cyclic strain for longer times, we found that the originally planar columnar epithelium spontaneously grew to form undulations and folds (Fig. 4a). When the vertical section was analyzed by immunofluorescence confocal microscopy, these folds were found to exhibit the morphology of normal intestinal villi lined by polarized columnar epithelial cells with basal nuclei and separated by crypts (Fig. 4b). The apical surfaces of epithelial cells within these villous structures stained positively for mucin 2, which is where this mucoprotein is deposited *in vivo*.[43] The timing of villi formation we observed in this *in vitro* model (on the order of weeks) is also consistent with the rate of villous renewal observed *in vivo*.[44,45] To our knowledge, spontaneous formation of intestinal villi by Caco-2 cells has never been reported previously, and this response which occurs after plating on planar ECM substrates appears to depend directly upon recapitulation of the mechanical microenvironment of the normal intestine that experiences low levels of fluid flow (and shear stress), as well as cyclic peristaltic motions.

Reconstitution of intestinal barrier functions *in vitro*

The Transwell model of intestinal epithelial barrier function that is often used as a tool for drug screening applications as well as cell biological studies,[8,46] involves culture of Caco-2 cells on a porous Transwell membrane, and tight junctional integrity is measured by quantifying TEER. We therefore compared TEER of Caco-2 monolayers grown under static Transwell conditions *versus* those that form in the gut-on-a-chip device with flow (30 μL h^{-1}) in the presence or absence of physiological cyclic strain (10%; 0.15 Hz). These studies revealed that cells grown under all three culture conditions increased their TEER over the first 6 days after plating and then maintained similar high levels for at least another 4 to 5 days of culture. However, cells in the microfluidic device with or without strain displayed peak TEER levels that were 3- to 4-fold higher than those of cells in static Transwell culture (Fig. 5a).

We also measured the apparent permeability coefficient (P_{app}) of the intestinal epithelium using fluorescent dextran (FD20), which characterizes the paracellular barrier function of intestinal epithelium due to pores associated with tight junctions.[35] We found that the P_{app} of cells was the same ($\sim 4 \times 10^{-8}$ cm s^{-1}) whether Caco-2 cells were cultured for 5 or 21 days in Transwell chambers (Fig. 5b). Cells cultured for 5 days in the microfluidic device with fluid flow alone (30 μL h^{-1}) also exhibited a similar P_{app}; however, additional application of cyclic mechanical strain (10% strain, 0.15 Hz + 30 μL h^{-1} flow) induced more than a 4-fold increase in paracellular permeability (Fig. 5b).

These results are consistent with published studies showing that Caco-2 cell monolayers in Transwell cultures display lower paracellular permeability values than those observed in human or animal intestine *in vivo*.[47–49] It has been proposed that this low level of permeability could result from the presence of a thick unstirred fluid layer in the static Transwell culture, which might limit diffusion.[50] One might then expect that fluid flow would increase paracellular permeability by producing fluid shear stress

Published on 08 March 2012 on http://pubs.rsc.org | doi:10.1039/C2LC40074J
Downloaded by UNIVERSITY OF SOUTH AUSTRALIA on 08 May 2012

This journal is © The Royal Society of Chemistry 2012

Downloaded by UNIVERSITY OF SOUTH AUSTRALIA on 08 May 2012
Published on 08 March 2012 on http://pubs.rsc.org | doi:10.1039/C2LC40074J

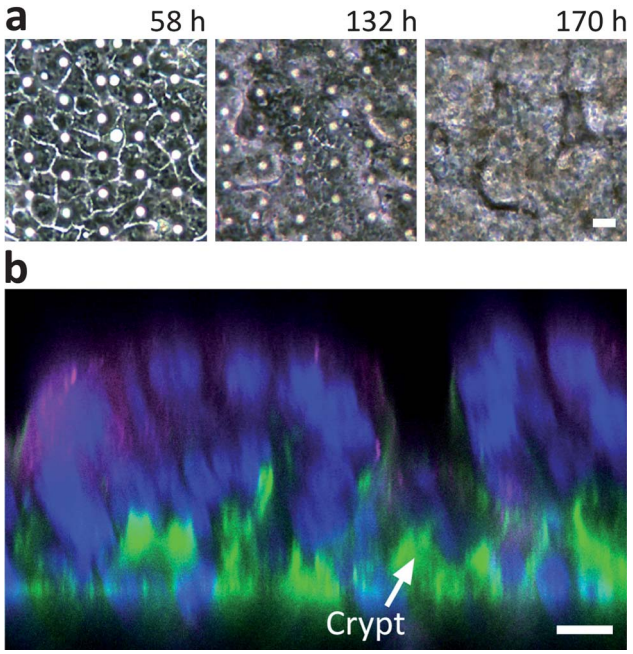


Fig. 4 Spontaneous formation of intestinal villi by Caco-2 cells cultured in the gut-on-a-chip. (**a**) Phase contrast views of a Caco-2 cell monolayer at 58, 132, and 170 h of culture in the presence of flow and cyclic strain (30 μL h^{-1}, 10% strain, 0.15 Hz). Note the planar epithelial monolayer visible at early times takes on an undulating quality with regions in and out of focus at later times that is suggestive of villi formation. (**b**) A confocal fluorescence view of a vertical cross section of a region of the undulating epithelium at 170 h confirming the presence of intestinal villi lined by consistently polarized columnar epithelial cells labeled with F-actin (green) with basal nuclei (blue) and apical mucin expression (magenta) separated by a crypt. The regular array of small white circles are pores visible beneath the epithelial monolayer; bar, 20 μm.

that decreases the thickness of the unstirred diffusion layer,[47,48,51] but fluid flow alone did not alter paracellular permeability in our system. Instead, we found that cyclic strain increased paracellular permeability, and this occurred under conditions that did not change TEER in these cell monolayers (Fig. 5b *vs.* 5a), suggesting that mechanical distortion might alter paracellular mechanisms of transport directly. Cyclic mechanical strain can increase transport of nanoparticles across lung epithelial and endothelial cell monolayers as a result of increased transcytosis,[25] and hence, it is possible that a similar mechanism could come into play here as well.

Next, we analyzed the catalytic activity of epithelial cell aminopeptidases to determine whether fluid flow and mechanical strain alter cytodifferentiation in human intestinal epithelial cells. Caco-2 cell differentiation measured by expression of aminopeptidase activity increased >7-fold over within cells cultured for 21 days compared to 5 days in the static Transwell system (Fig. 5c), which is consistent with previously published findings.[52] Importantly, culture of cells under fluid flow (30 μL h^{-1}) in the microfluidic device greatly accelerated this response, producing almost a 9-fold increase in aminopeptidase activity after only 5 days in culture, and an even greater increase was produced when cells were grown in the gut-on-a-chip that applies the same fluid flow and cyclic mechanical strain (10% strain, 0.15 Hz) simultaneously. These results are consistent with a past study which showed that cyclic strain can similarly increase expression of expression of intestinal differentiation-specific enzyme activities in Caco-2 cells.[29]

Host-microflora co-culture

One of the most crucial components of human gut physiology that has never been modeled effectively *in vitro* is the normal presence of microbial communities in the lumen of the gut.[53] To explore whether the highly differentiated intestinal epithelium produced in the gut-on-a-chip could support co-culture of microbial flora, we cultured the normal intestinal microbe, *Lactobacillus rhamnosus* GG (LGG), on the apical surface of Caco-2 cell monolayer, and cells cultured in Transwell chambers under static conditions were used as controls. After microfluidic co-culture with continuous flow (40 μL h^{-1})

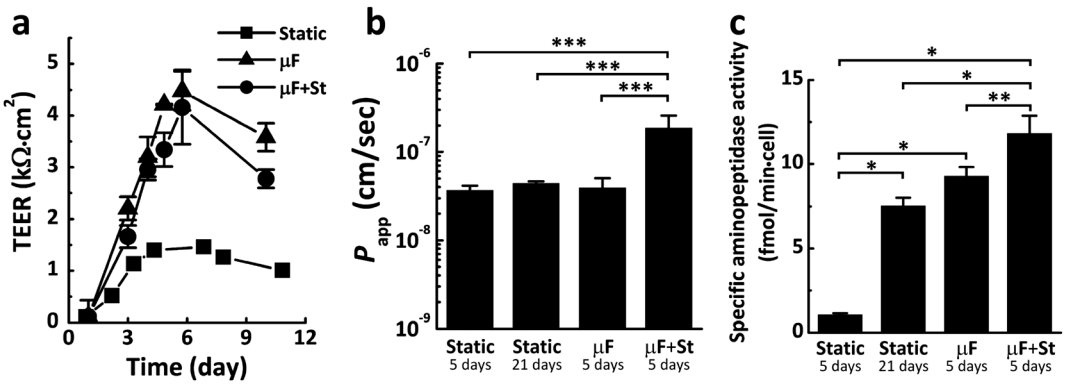


Fig. 5 Evaluation of intestinal barrier functions and differentiation of a Caco-2 monolayer cultured in either the Transwell (Static) or the microfluidic gut-on-a-chip in the absence (μF) or presence (μF + St) of cyclic strain. (**a**) Tight junctional integrity of the epithelium quantified by measuring TEER of the Caco-2 monolayer. (**b**) Apparent paracellular permeability (P_{app}) measured by quantitating fluorescent dextran transport through the Caco-2 monolayer cultured under static conditions for 5 or 21 days, or in the microfluidic gut-on-a-chip in the absence (μF) or presence (μF + St) of cyclic strain for 5 days (*** $p < 0.05$). (**c**) Intestinal cell differentiation assessed by measuring brush border aminopeptidase activity in Caco-2 cells cultured under static conditions for 5 or 21 days, or in the microfluidic gut-on-a-chip in the absence (μF) or presence (μF + St) of cyclic strain for 5 days (* $p < 0.001$, ** $p < 0.01$).

Published on 08 March 2012 on http://pubs.rsc.org | doi:10.1039/C2LC40074J
Downloaded by UNIVERSITY OF SOUTH AUSTRALIA on 08 May 2012

and cyclic strain (10%, 0.15 Hz) for 96 h, microcolonies of LGG cells still remained tightly adherent to the surface of a Caco-2 monolayer (Fig. 6a). Live/dead staining of the culture with calcein-AM and ethidium homodimer-1, respectively, confirmed that the Caco-2 epithelial cells remained fully (>95%) viable after co-culture with LGG under these conditions (Fig. 6b). LGG express a bacterial-specific β-galactosidase activity when grown alone in culture whereas this is not expressed by intestinal epithelial cells (Fig. S2). When we measured β-galactosidase activity in the top chamber of the co-cultures, it too remained high, thus confirming that the LGG cells also remained viable under these culture conditions (Fig. 6d).

Importantly, not only was the intestinal cell monolayer able to maintain normal barrier functions under these co-culture conditions with living microbes growing on its apical surface, barrier integrity measured by quantitating TEER actually improved over time (Fig. 6c). This result is consistent with the finding that probiotic strains of bacteria, including LGG, have been reported to increase intestinal epithelial integrity *in vitro*[54] and enhance intestinal barrier function in humans.[55] In contrast, TEER dissipated over the first day of co-culture in the static Transwell system and could not be measured at all after 48 h (Fig. 6c) due to death and complete detachment of the epithelial monolayer.

The human microbiome plays a central role in intestinal health and disease,[20,56,57] and so development of an *in vitro* platform to study host-microbe interplay should be of great interest to cell biologists and physiologists, as well as pharmaceutical scientists.[58,59] Past studies have carried out short-term co-culture of intestinal epithelial cells with living bacteria to study microbial adherence,[60] invasion,[61] translocation,[62] and biofilm formation.[63] But long-term co-culture of microbes with host cells has not been possible due to microbial overgrowth and loss of epithelial viability. This is likely due to difficulties in matching growth conditions between the host cell and microbe,[63] controlling the population density of microbes in antibiotic-free culture condition,[64] or restricting production of metabolites (*e.g.* organic acids) by microbial cells.[65,66] We also found that LGG cells grew without constraint in the stagnant apical chamber of the Transwell system, causing drastic decrease of medium pH (pH 2.5–3.0) that is not consistent with intestinal epithelial cell survival (not shown). Importantly, however, the microfluidic nature of the gut-on-a-chip provides a way to overcome this challenge because it effectively functions as a continuous flow bioreactor. Specifically, the dilution rate of the culture medium in gut-on-a-chip (~8.0 h^{-1}) is much higher than the specific growth rate of LGG in the culture medium (~0.2 h^{-1}), which permits clearance of organic acids and unbound LGG cells. LGG cells that were tightly adherent on the surface of a Caco-2 monolayer remained in the gut-on-a-chip device while all non-adherent LGG cells were washed out, which prevented unrestrained overgrowth of the cultures. Given that intestinal epithelial integrity significantly increased in the presence of LGG co-cultures, the presence of microbes apparently provides normal microenvironmental cues that enhance epithelial cell functions (*e.g.* mucin secretion) that are necessary to maintain this dynamic interface, which is consistent human clinical studies.[55]

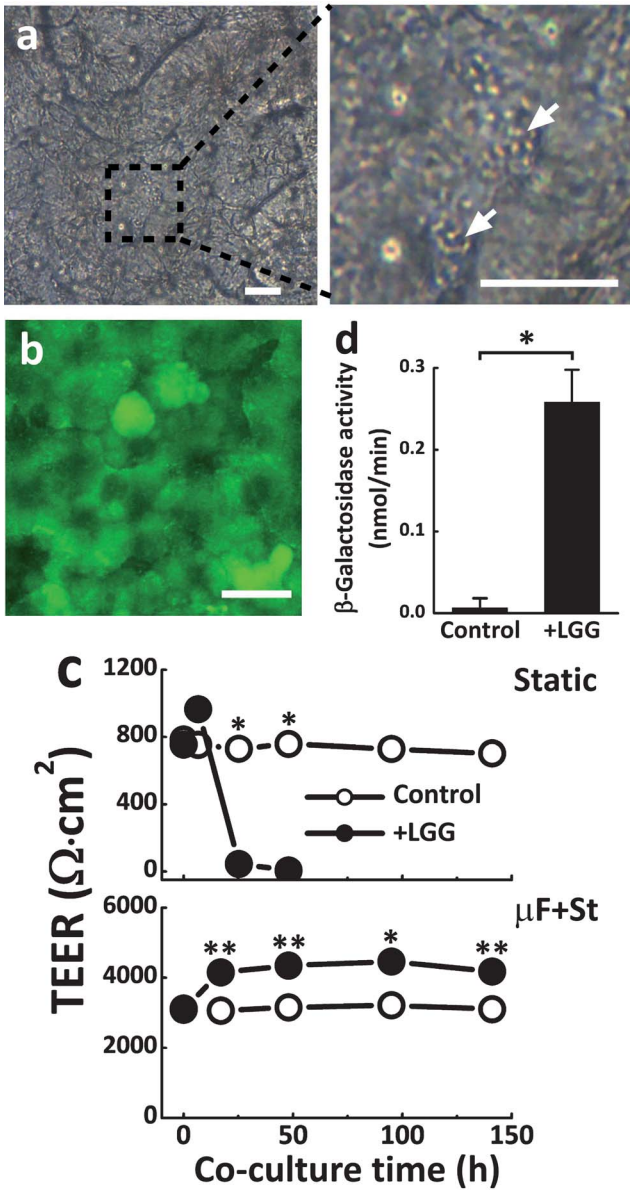


Fig. 6 Long-term microbial co-culture on a human intestinal epithelial monolayer in the gut-on-a-chip. A bacterium originally isolated from human intestine, *Lactobacillus rhamnosus* GG (LGG), was cultured on the surface of a Caco-2 monolayer grown within the gut-on-a-chip. (**a**) Phase contrast views from above of LGG and Caco-2 cells co-cultured for 96 h and viewed at low (left) and high (right) magnification, which show microcolonies of LGG cells (white arrows) that remain tightly adherent to the apical surface of the Caco-2 cell monolayer after exposure to continuous fluidic flow (bar, 20 μm in all views). (**b**) Simultaneous live/dead staining of a Caco-2 monolayer co-cultured with LGG for 96 h demonstrating that virtually all epithelial cells remained viable (green). (**c**) Barrier functions of the Caco-2 monolayer cultured in the absence (open circles) or presence (closed circles) of LGG cells in Transwell (Static) or microfluidic gut-on-a-chip with cyclic strain (μF + St; 40 μL h^{-1}, 10% cell strain, 0.15 Hz). Note that error bars were smaller than the symbol size (* $p < 0.01$, ** $p < 0.05$). (**d**) Assessment of the functionality of viable LGG cells co-cultured with Caco-2 cells for 96 h carried out by measuring the catalytic activity of β-galactosidases in LGG cells co-cultured with Caco-2 cells in gut-on-a-chip with mechanical strain (+LGG; 40 μL h^{-1}, 10% cell strain, 0.15 Hz) or in Caco-2 cells cultured alone as a control (*$p < 0.01$).

This journal is © The Royal Society of Chemistry 2012

Published on 08 March 2012 on http://pubs.rsc.org | doi:10.1039/C2LC40074J
Downloaded by UNIVERSITY OF SOUTH AUSTRALIA on 08 May 2012

Conclusion

The human gut-on-a-chip microdevice provides a controlled microplatform to study and perturb critical gut functions in the presence of relevant physiological cues, including cyclic mechanical strain, fluid flow and coexistence of microbial flora. Characterization of this device revealed that recapitulating the low level of fluid flow and shear stress experienced in the living intestine is sufficient to promote accelerated intestinal epithelial cell differentiation, formation of 3D villi-like structures, and increased intestinal barrier function, and that addition of cyclic mechanical strain that mimics normal peristaltic motions further enhances these responses. Moreover, once differentiated within the gut-on-a-chip device, the intestinal epithelium can support growth of microbial flora that normally lives within the human intestine. The human peristaltic gut-on-a-chip may therefore facilitate study of mechanoregulation of intestinal function, as well as host-microbe symbiosis and evolution. Given that it effectively recapitulates many complex functions of the normal human intestine, it also may become an essential platform for drug screening and toxicology testing.

Acknowledgements

This work was supported by the Wyss Institute for Biologically Inspired Engineering at Harvard University and by a grant from NIEHS (ES016665-01A1).

References

1 J. C. Davila, R. J. Rodriguez, R. B. Melchert and D. Acosta Jr., *Annu. Rev. Pharmacol.*, 1998, **38**, 63–96.
2 J. A. Kramer, J. E. Sagartz and D. L. Morris, *Nat. Rev. Drug Discovery*, 2007, **6**, 636–649.
3 H. Olson, G. Betton, D. Robinson, K. Thomas, A. Monro, G. Kolaja, P. Lilly, J. Sanders, G. Sipes, W. Bracken, M. Dorato, K. Van Deun, P. Smith, B. Berger and A. Heller, *Regul. Toxicol. Pharmacol.*, 2000, **32**, 56–67.
4 K. M. Giacomini, S. M. Huang, D. J. Tweedie, L. Z. Benet, K. L. R. Brouwer, X. Y. Chu, A. Dahlin, R. Evers, V. Fischer, K. M. Hillgren, K. A. Hoffmaster, T. Ishikawa, D. Keppler, R. B. Kim, C. A. Lee, M. Niemi, J. W. Polli, Y. Sugiyama, P. W. Swaan, J. A. Ware, S. H. Wright, S. W. Yee, M. J. Zamek-Gliszczynski, L. Zhang and T. International, *Nat. Rev. Drug Discovery*, 2010, **9**, 215–236.
5 J. Hodgson, *Nat. Biotechnol.*, 2001, **19**, 722–726.
6 E. Le Ferrec, C. Chesne, P. Artusson, D. Brayden, G. Fabre, P. Gires, F. Guillou, M. Rousset, W. Rubas and M. L. Scarino, *Atla-Altern. Lab. Anim.*, 2001, **29**, 649–668.
7 I. D. Angelis and L. Turco, *Current protocols in toxicology/editorial board*, Mahin D. Maines (editor-in-chief). [*et al.*], 2011, Chapter 20.
8 K.-J. Kim, in *Cell Culture Models of Biological Barriers*, ed. C.-M. Lehr, Taylor & Francis, New York, 2002, pp. 41–51.
9 I. J. Hidalgo, T. J. Raub and R. T. Borchardt, *Gastroenterology*, 1989, **96**, 736–749.
10 G. J. Mahler, M. B. Esch, R. P. Glahn and M. L. Shuler, *Biotechnol. Bioeng.*, 2009, **104**, 193–205.
11 J. H. Sung, J. J. Yu, D. Luo, M. L. Shuler and J. C. March, *Lab Chip*, 2011, **11**, 389–392.
12 J. H. Sung, C. Kam and M. L. Shuler, *Lab Chip*, 2010, **10**, 446–455.
13 H. Kimura, T. Yamamoto, H. Sakai, Y. Sakai and T. Fujii, *Lab Chip*, 2008, **8**, 741–746.
14 Y. Imura, Y. Asano, K. Sato and E. Yoshimura, *Anal. Sci.*, 2009, **25**, 1403–1407.
15 I. R. Sanderson, *Am. J. Clin. Nutr.*, 1999, **69**, 1028S–1034S.
16 C. P. Gayer and M. D. Basson, *Cell. Signal.*, 2009, **21**, 1237–1244.
17 M. D. Basson and C. P. Coppola, *Metab., Clin. Exp.*, 2002, **51**, 1525–1527.
18 H. Kehlet and K. Holte, *Am. J. Surg.*, 2001, **182**, S3–10S.
19 J. E. Kellow and S. F. Phillips, *Gastroenterology*, 1987, **92**, 1885–1893.
20 L. V. Hooper, *Trends Microbiol.*, 2004, **12**, 129–134.
21 J. C. Arthur and C. Jobin, *Inflammatory Bowel Dis.*, 2011, **17**, 396–409.
22 H. Sokol and P. Seksik, *Curr. Opin. Gastroenterol.*, 2010, **26**, 327–331.
23 J. L. Round and S. K. Mazmanian, *Nat. Rev. Immunol.*, 2009, **9**, 313–323.
24 J. R. Turner, *Nat. Rev. Immunol.*, 2009, **9**, 799–809.
25 D. Huh, B. D. Matthews, A. Mammoto, M. Montoya-Zavala, H. Y. Hsin and D. E. Ingber, *Science*, 2010, **328**, 1662–1668.
26 K. J. Jang and K. Y. Suh, *Lab Chip*, 2010, **10**, 36–42.
27 K. J. Jang, H. S. Cho, H. Kang do, W. G. Bae, T. H. Kwon and K. Y. Suh, *Integr. Biol.*, 2011, **3**, 134–141.
28 M. D. Peterson and M. S. Mooseker, *J. Cell Sci.*, 1992, **102**(Pt 3), 581–600.
29 M. D. Basson, G. D. Li, F. Hong, O. Han and B. E. Sumpio, *J. Cell. Physiol.*, 1996, **168**, 476–488.
30 J. H. Zhang, W. Li, M. A. Sanders, B. E. Sumpio, A. Panja and M. D. Basson, *FASEB J.*, 2003, **17**, 926.
31 M. D. Basson, G. Turowski and N. J. Emenaker, *Exp. Cell Res.*, 1996, **225**, 301–305.
32 M. D. Basson, *Digestion*, 2003, **68**, 217–225.
33 M. Furuse, T. Hirase, M. Itoh, A. Nagafuchi, S. Yonemura and S. Tsukita, *J. Cell Biol.*, 1993, **123**, 1777–1788.
34 C. Piana, I. Gull, S. Gerbes, R. Gerdes, C. Mills, J. Samitier, M. Wirth and F. Gabor, *Differentiation*, 2007, **75**, 308–317.
35 I. Hubatsch, E. G. Ragnarsson and P. Artursson, *Nat. Protoc.*, 2007, **2**, 2111–2119.
36 M. Saxelin, *Food Rev. Int.*, 1997, **13**, 293–313.
37 L. G. Durrant, E. Jacobs and M. R. Price, *Eur. J. Cancer*, 1994, **30**, 355–363.
38 R. G. Lentle and P. W. M. Janssen, *J. Comp. Physiol., B*, 2008, **178**, 673–690.
39 S. P. Olesen, D. E. Clapham and P. F. Davies, *Nature*, 1988, **331**, 168–170.
40 T. Ishikawa, T. Sato, G. Mohit, Y. Imai and T. Yamaguchi, *J. Theor. Biol.*, 2011, **279**, 63–73.
41 T. F. Bullen, S. Forrest, F. Campbell, A. R. Dodson, M. J. Hershman, D. M. Pritchard, J. R. Turner, M. H. Montrose and A. J. Watson, *Lab. Invest.*, 2006, **86**, 1052–1063.
42 G. Wilson, I. F. Hassan, C. J. Dix, I. Williamson, R. Shah, M. Mackay and P. Artursson, *J. Controlled Release*, 1990, **11**, 25–40.
43 S. B. Ho, G. A. Niehans, C. Lyftogt, P. S. Yan, D. L. Cherwitz, E. T. Gum, R. Dahiya and Y. S. Kim, *Cancer Res.*, 1993, **53**, 641–651.
44 E. Marshman, C. Booth and C. S. Potten, *BioEssays*, 2002, **24**, 91–98.
45 F. Radtke and H. Clevers, *Science*, 2005, **307**, 1904–1909.
46 P. Shah, V. Jogani, T. Bagchi and A. Misra, *Biotechnol. Prog.*, 2006, **22**, 186–198.
47 A. Avdeef and K. Y. Tam, *J. Med. Chem.*, 2010, **53**, 3566–3584.
48 H. Lennernas, K. Palm, U. Fagerholm and P. Artursson, *Int. J. Pharm.*, 1996, **127**, 103–107.
49 S. Y. Yee, *Pharm. Res.*, 1997, **14**, 763–766.
50 I. J. Hidalgo, K. M. Hillgren, G. M. Grass and R. T. Borchardt, *Pharm. Res.*, 1991, **8**, 222–227.
51 H. Lennernas, *Xenobiotica*, 2007, **37**, 1015–1051.
52 S. Howell, A. J. Kenny and A. J. Turner, *Biochem. J.*, 1992, **284**, 595–601.
53 F. Shanahan, *Best Pract. Res. Clin. Gastroenterol.*, 2002, **16**, 915–931.
54 H. W. Fang, S. B. Fang, J. S. C. Chiau, C. Y. Yeung, W. T. Chan, C. B. Jiang, M. L. Cheng and H. C. Lee, *J. Med. Microbiol.*, 2010, **59**, 573–579.
55 C. Dai, D.-H. Zhao and M. Jiang, *Int. J. Mol. Med*, 2012, **29**, 202–208.
56 P. J. Turnbaugh, R. E. Ley, M. Hamady, C. M. Fraser-Liggett, R. Knight and J. I. Gordon, *Nature*, 2007, **449**, 804–810.
57 F. H. Karlsson, I. Nookaew, D. Petranovic and J. Nielsen, *Trends Biotechnol.*, 2011, **29**, 251–258.
58 J. K. Nicholson, E. Holmes and I. D. Wilson, *Nat. Rev. Microbiol.*, 2005, **3**, 431–438.
59 P. W. Lin, T. R. Nasr, A. J. Berardinelli, A. Kumar and A. S. Neish, *Pediatr. Res.*, 2008, **64**, 511–516.
60 G. Chauviere, M. H. Coconnier, S. Kerneis, J. Fourniat and A. L. Servin, *J. Gen. Microbiol.*, 1992, **138**, 1689–1696.

61 M. H. Coconnier, M. F. Bernet, S. Kerneis, G. Chauviere, J. Fourniat and A. L. Servin, *FEMS Microbiol. Lett.*, 1993, **110**, 299–305.
62 P. Harvey, T. Battle and S. Leach, *J. Med. Microbiol.*, 1999, **48**, 461–469.
63 J. Kim, M. Hegde and A. Jayaraman, *Lab Chip*, 2010, **10**, 43–50.
64 G. Zoumpopoulou, E. Tsakalidou, J. Dewulf, B. Pot and C. Grangette, *Int. J. Food Microbiol.*, 2009, **131**, 40–51.
65 M. Moussavi and M. C. Adams, *Curr. Microbiol.*, 2010, **60**, 327–335.
66 H. Annuk, J. Shchepetova, T. Kullisaar, E. Songisepp, M. Zilmer and M. Mikelsaar, *J. Appl. Microbiol.*, 2003, **94**, 403–412.

Downloaded by UNIVERSITY OF SOUTH AUSTRALIA on 08 May 2012
Published on 08 March 2012 on http://pubs.rsc.org | doi:10.1039/C2LC40074J

This journal is © The Royal Society of Chemistry 2012